

THE DAMAGE PROCESS IN A FINITE-SIZED BRITTLE SPECIMEN WITH INTERACTING MICROCRACKS

A. CARPINTERI and G. P. YANG*

Department of Structural Engineering, Politecnico di Torino, 10129 Torino, Italy

Abstract—The whole damage process in a finite sized specimen with interacting microcracks is simulated by a method combining the closed form crack solutions with boundary elements. Interactions among microcracks and boundary elements are taken into account with an explicit interaction matrix. A coalescence criterion is assumed to rule the intersection behaviour and propagation arrest. The fatal coalescence cluster resulting in the failure of the specimen, out of many intersections of propagating microcracks, is identified with a particular coalescence matrix. The numerical model proposed in this paper can be used to simulate the damage process in a brittle specimen of any shape, under arbitrary plane stress conditions.

Keywords—Brittle materials; Crack propagation; Crack interactions; Boundary elements.

NOMENCLATURE

- a = microcrack length
- C_{ij}^{pp} , C_{ij}^{pa} , C_{ij}^{ap} , C_{ij}^{aa} = influence coefficients of stresses at point j on those at point i in boundary elements
- k_{12}^n , k_{12}^s , k_{21}^n , k_{21}^s = influence vectors corresponding to the stress field generated by unit normal or shear stresses on the interacting microcrack
- K^o = SIF corresponding to the applied boundary stresses
- K^{Add} = SIF corresponding to the additional interaction stresses
- O, S = opening and sliding forces on the branching crack generated by fictitious stresses
- $p1(x1)$, $p2(x2)$, $s1(x1)$, $s2(x2)$ = fictitious normal and shear stresses on microcracks
- R_{12}^{pp} , R_{12}^{pa} , R_{12}^{ap} , R_{12}^{aa} = interaction coefficients between microcracks
- $R_{1,j}$ = interaction submatrix of source microcrack J on microcrack I
- R_{ik}^{pp} , R_{ik}^{pa} , R_{ik}^{ap} , R_{ik}^{aa} = influence coefficients of microcrack k on microcrack i with three points stress assumption
- θ = microcrack orientation
- λ = friction coefficient between the two crack surfaces in compression
- σ, τ = general normal and shear stresses
- σ_{mi} = fictitious stress vector on microcrack surface
- σ_{mi}^{bound} = stress generated only by the boundary stresses
- σ_{mi}^{inter} = additional stress generated by the microcrack interaction
- σ_{12} = stress vector acting on microcrack 1 induced by microcrack 2
- σ_{21} = stress vector acting on microcrack 2 induced by microcrack 1

INTRODUCTION

The failure process in brittle materials is the result of the propagation, coalescence and interaction of many pre-existing microcracks or voids. Micromechanics of imperfections in brittle materials has become a very important research topic in civil engineering investigations. Many researchers have studied the fracture behaviour in brittle materials with interacting microcracks [1–3] (mostly based on the infinite size assumption) without considering the boundary influence on the fracture

*On leave from the Dept. of Civil Engineering, Tsinghua University, Beijing, China.

behaviour. In real situations however, brittle materials present finite size boundaries and the specimen size has a very large influence on the loading capacity. When simulating the complex damage mechanisms in brittle materials with a multitude of randomly distributed microcracks, it is necessary to include the finite sized boundary effects in microcrack interaction and propagation behaviour during the loading process.

On the basis of our previous simple microcrack interaction and propagation model for infinite sized plates [4,5], the boundary element method is applied to take into account the effects of finite sized boundaries. Interactions among microcracks and boundary elements are therefore formulated with an explicit interaction matrix. The brittle specimen is represented with an arbitrary sized plate with a multitude of randomly distributed microcracks. The load is divided into several increments and in each load increment the microcrack interaction and propagation together with the influence of the finite boundary on the fracture behaviour of microcracks are followed progressively. For computational convenience and accuracy, a microcrack is discretized with six degrees of freedom, which enables us to describe any possible crack propagation configuration, from initial branching to asymmetric propagation due to the interaction effects. During crack propagation, the microcracks may coalesce and intersect each other, and some microcracks will be arrested, so a coalescence criterion is needed to check the intersection behaviour and to decide the propagation arrest of the less important intersecting cracks. The judgment whether the specimen is in the failure stage is accomplished by a particular coalescence matrix which allows us to find the fatal coalescence cluster out of many intersections of propagating microcracks.

CRACK INTERACTION CONSIDERATIONS

Basic formulation

It is very convenient to adopt the fictitious stress concept for the computation of Stress Intensity Factors (SIFs) in crack interaction situations. The fictitious stresses are assumed as the on-site stresses acting on the microcrack surfaces even though the crack surfaces are stress-free. For the stress distribution around a crack, whose surfaces are subjected to uniform normal or shear stresses, Sneddon and Lowengrub [6] obtained the closed form solutions. Such exact solutions have been used to compute the SIFs of microcracks with crack interaction [4,7]. The results are in good agreement with some typical problems where closed solutions exist.

In this paper, two algorithms are adopted in computing the SIFs of microcracks in interaction and propagation. The exact solutions by Sneddon and Lowengrub are used for original microcracks (i.e. those that have not propagated), which allow us to get good estimations for the start of crack propagation and crack branching directions. After the crack has propagated, the approximate K -dominant stress field, commonly used in classical fracture mechanics, is adopted.

If an external stress field is applied to the specimen, the fictitious stress σ_{mi} on the microcrack surfaces is composed of two parts

$$\sigma_{mi} = \sigma_{mi}^{\text{bound}} + \sigma_{mi}^{\text{inter}} \quad (1)$$

The first term, $\sigma_{mi}^{\text{bound}}$, is the stress field generated only by the boundary stresses, while the second term, $\sigma_{mi}^{\text{inter}}$, is the additional stress field generated by the microcrack interaction. These two parts can be found when solving the problem. We will focus our attention on the second part due to crack interaction, whereas the first part will be discussed in the following section within the boundary element method framework.

Considering boundary effects and crack interactions, the SIFs of the microcrack tips can be expressed as

$$K_I = K_I^o + K_I^{Add}, \quad K_{II} = K_{II}^o + K_{II}^{Add} \tag{2}$$

in which K^o and K^{Add} are SIFs corresponding to the applied boundary stresses and to the additional stresses generated by the crack interaction, respectively.

To make the formulation of the crack interaction process clearer, only two microcracks are considered. Thus the existence of two microcracks with arbitrary sizes and arbitrary orientations, $a_1, a_2, \theta_1, \theta_2$, are shown in Fig. 1(a), with a set of boundary stresses acting on the specimen. This fundamental problem can be split into three sub-problems as shown in Fig. 1(b), where subscripts 1 and 2 represent the parameters corresponding to microcrack 1 and 2, respectively. Stresses σ_1^{bound} and σ_2^{bound} are the stress vectors acting on the microcracks 1 and 2 and induced by the boundary stresses, while σ_{12} is the stress vector acting on microcrack 1 induced by microcrack 2. The surfaces of the latter are subjected to the stress vector $-(\sigma_2^{bound} + \sigma_{21})$, where the stress vector σ_{21} is that induced by microcrack 1 on microcrack 2. The surfaces of the former, on the other hand, are subjected to the stress vector $-(\sigma_1^{bound} + \sigma_{12})$.

The problem focuses on finding these stress vectors caused by the boundary stresses and the interaction effects between the two cracks. If the final fictitious normal stress and shear stress on microcrack 1 are denoted, on the crack line coordinate x_1 , as $p_1(x_1)$ and $s_1(x_1)$,

$$p_1(x_1) = -p_1^{bound} - n_1 \sigma_{12} n_1, \quad s_1(x_1) = -s_1^{bound} - n_1 \sigma_{12} t_1 \tag{3}$$

where p_1^{bound} and s_1^{bound} are the normal and shear stresses induced by the boundary load, n_1 and t_1 are direction cosines of microcrack 1 related to the local coordinates of the microcrack 2, and the stress vector σ_{12} is also related to this local system.. The stresses $p_2(x_2)$ and $s_2(x_2)$ on the

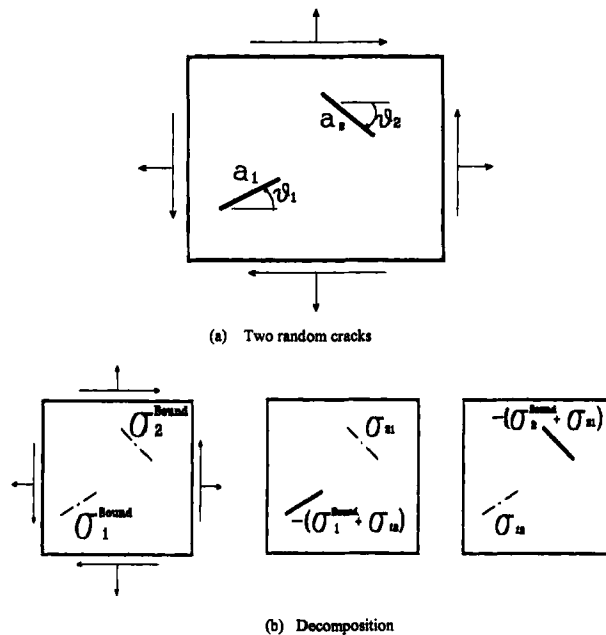


Fig. 1. Two cracks in a finite sized plate and their decomposition.

surface of microcrack 2 are analogously given by

$$p_2(x_2) = -p_2^{\text{bound}} - n_2 \sigma_{21} n_2, \quad s_2(x_2) = -s_2^{\text{bound}} - n_2 \sigma_{21} t_2 \tag{4}$$

in which n_2 and t_2 are the direction cosines of microcrack 2. Let us distinguish the individual contributions of normal and shear stresses to the additional stress vectors

$$\sigma_{12} = k_{12}^p p_2(x_2) + k_{12}^s s_2(x_2), \quad \sigma_{21} = k_{21}^p p_1(x_1) + k_{21}^s s_1(x_1) \tag{5}$$

in which $k_{12}^p, k_{12}^s, k_{21}^p, k_{21}^s$ are the influence vectors corresponding to the stress field generated by unit normal or shear stresses on the interacting microcrack. In numerical computation, stresses are only computed at some special points on the microcracks, so that the stresses at certain points can be expressed as

$$\begin{aligned} p_1 &= -p_1^{\text{bound}} - R_{12}^{pp} p_2 - R_{12}^{ps} s_2, & s_1 &= -s_1^{\text{bound}} - R_{12}^{sp} p_2 - R_{12}^{ss} s_2 \\ p_2 &= -p_2^{\text{bound}} - R_{21}^{pp} p_1 - R_{21}^{ps} s_1, & s_2 &= -s_2^{\text{bound}} - R_{21}^{sp} p_1 - R_{21}^{ss} s_1 \end{aligned} \tag{6}$$

where $R_{12}^{pp}, R_{12}^{ps}, R_{12}^{sp}, R_{12}^{ss}, \dots$ represent the interaction coefficients between the microcracks. To extend the procedure to the multi-microcrack situation, where there are M microcracks in the specimen, the problem can also be separated into $M + 1$ sub-problems presenting the same formulation steps as those in the case of two microcracks,

$$p_i = -p_i^{\text{bound}} - \sum_{k \neq i}^M [R_{ik}^{pp} p_k + R_{ik}^{ps} s_k], \quad s_i = -s_i^{\text{bound}} - \sum_{k \neq i}^M [R_{ik}^{sp} p_k + R_{ik}^{ss} s_k] \tag{7}$$

Equation (7) represents $2M$ linear relations for solving $2M$ unknowns $p_1, s_1, \dots, p_m, s_m$. In the next section six degrees of freedom will be used to represent a crack stress state and to simulate the various crack configurations during propagation.

Crack interaction during propagation

Microcracks during propagation can be grouped into four types as shown in Fig. 2, according to the possible different branching configurations. The stress distribution for the different types of microcrack and the stresses acting on microcracks should be evaluated differently. In the formulation procedure, two main steps are the treatment of stresses on the microcrack (referred to as the target microcrack) caused by other interacting microcracks (referred to as the source microcracks), and the evaluation of the stress field generated by source microcracks.

To model the variation of the stresses on a target microcrack generated by other source microcracks, normal and shear stresses at three points on each target microcrack are computed to evaluate the SIFs at the two tips of the crack, the choice of the three points on the target crack is dependent on the different propagation patterns of the crack. While the first point is always located at the center of the original crack, the other two points are chosen according to the propagation states of the two tips.

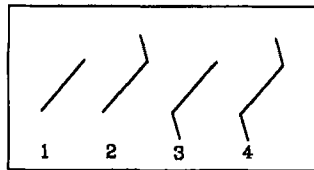


Fig. 2. Different crack patterns during propagation.

If the two tips have not propagated (type 1) the other two points are located in the two tips of the original crack, so that the three point stresses on this unpropagated crack can give out a quadratic stress distribution to determine more effectively the initiation of the branching cracks. If only one tip of the original crack has propagated (type 2 or type 3), then one point is located at the tip of the original crack and the other at the center of the branching crack. If both tips have propagated (type 4), the two points are located at the centers of the two branching cracks, respectively.

The formulation procedure relating to the stress field yielded by source microcracks is more complicated. The simplest case is that of the type 1 crack with two unpropagated tips. The final stresses, including the contributions of other interacting cracks, at three points of this crack result in a quadratic distribution, and the stress field near this crack is obtainable from the solutions given by Sneddon and Lowengrub [6]. For the type 2 and type 3 cracks, the stress field should be composed of that from an unpropagated original crack tip and that from a branched crack tip. The SIF at the unpropagated tip should be computed from the linearly varied stresses on the original crack resulting from the two point stresses.

In the case of the type 4 crack with both tips propagated, the SIFs at each of the branching crack tips should take into account the opening and sliding forces caused by the constant stress on the original crack and the contribution of the stresses on branching cracks, as will be described in a later section.

Since six stresses at the three characteristic points of a microcrack should be always considered for different configurations, the influence matrix expressed in Eq. (7) should be extended to be compatible with the six degrees of freedom of each microcrack. For the contributions of the source microcrack J to the stresses on the target microcrack I , corresponding submatrices take the following form

$$R_{I,J} = \begin{bmatrix} R_{6 \times 1 - 5, 6 \times J - 5} & R_{6 \times 1 - 5, 6 \times J - 4} & \dots & \dots & \dots \\ R_{6 \times 1 - 4, 6 \times J - 5} & R_{6 \times 1 - 4, 6 \times J - 4} & \dots & \dots & \dots \\ \dots & \dots & \dots & \dots & \dots \\ \dots & \dots & \dots & R_{6 \times 1, 6 \times J - 1} & R_{6 \times 1, 6 \times J} \end{bmatrix} \quad (8)$$

Now the interaction matrix is $6M \times 6M$ when M microcracks are in the specimen. Combining this matrix with the boundary elements described below, final fictitious stresses on each microcrack can be obtained after solving the interaction problem. The propagation conditions and the lengths of the branching cracks can be computed or checked according to the above criteria, step by step along with the increment of the external loads.

BOUNDARY INFLUENCE ON MICROCRACKS

The previous formulation procedures are based on the solution of cracks in an infinite elastic domain. To take account of the influence of a finite sized boundary, a boundary element method is introduced. The framework of the Fictitious Stress Method (FSM) [8,9] is in accordance with our former formulations since in both of them the unknowns are the stresses deduced from the other stress sources.

FSM is based on the exact solution of a point force acting on an infinite plane. A fictitious stress is assumed to act on the discrete boundary element, which is called the Stress Discontinuity (SD) element since there exists a stress jump on both sides of the element. Over each element, the stress discontinuities are assumed to vary according to a given mode (constant, linear, etc.), then

the normal and shear stresses p_i and s_i generated by N discrete SD elements are

$$p_i = \sum_{j=1}^N C_{ij}^{pp} p_j + \sum_{j=1}^N C_{ij}^{ps} s_j, \quad s_i = \sum_{j=1}^N C_{ij}^{sp} p_j + \sum_{j=1}^N C_{ij}^{ss} s_j \quad (9)$$

where p_j, s_j are the unknown normal and tangential Stress Discontinuities at the mid-point of the boundary elements, C_{ij}^{pp}, C_{ij}^{ps} , etc. are the influence coefficients of stresses at point j on those at point i .

In the case of cracks in a finite sized body, we can divide the external boundary into N Stress Discontinuity elements, which, with M internal microcracks, provide the following $2N + 6M$ algebraic equations:

$$p_i = - \sum_{j=1}^N [C_{ij}^{pp} p_j + C_{ij}^{ps} s_j] - \sum_{k \neq i}^M \sum_{l=1}^3 [R_{ikl}^{pp} p_{k_l} + R_{ikl}^{ps} s_{k_l}] \quad (10)$$

$$s_i = - \sum_{j=1}^N [C_{ij}^{sp} p_j + C_{ij}^{ss} s_j] - \sum_{k \neq i}^M \sum_{l=1}^3 [R_{ikl}^{sp} p_{k_l} + R_{ikl}^{ss} s_{k_l}]$$

This equation enables us to determine $2N$ Stress Discontinuity unknowns and $6M$ fictitious stresses for M microcracks, and then to evaluate the SIF at every microcrack tip with a different propagation configuration in a finite sized plate.

SIF EVALUATION AND CRACK PROPAGATION MODEL

After getting the fictitious stresses on each microcrack, the SIFs are evaluated and the propagation states can be checked in the case of mixed mode fracture.

Specimen in tension

Suppose that there is only a preexisting crack of length a_i under a mixed mode loading condition as shown in Fig. 3(a); the SIFs at its tips are assumed to be K_I and K_{II} , respectively.

From the well-known maximum hoop stress criterion, the crack tip j ($j = 1, 2$) will begin propagating when

$$\cos \frac{\theta_{ij}}{2} \left[K_I \cos^2 \frac{\theta_{ij}}{2} - \frac{3}{2} K_{II} \sin \theta_{ij} \right] = K_{IC} \quad (11)$$

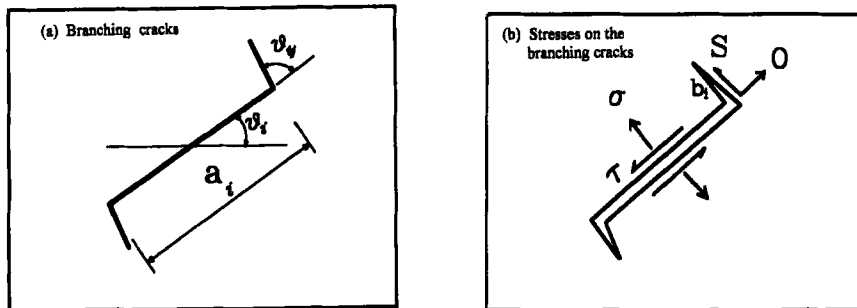


Fig. 3. A crack in a branched configuration.

where K_{IC} is the mode I fracture toughness of the material, and the propagation angle θ_{ij} , which is the value corresponding to the tip j of the crack i , satisfies the condition

$$K_I \sin \theta_{ij} + K_{II}(3 \cos \theta_{ij} - 1) = 0 \tag{12}$$

When the microcrack interaction effect is not considered, the two angles θ_{i1} and θ_{i2} are equal, but when considering crack interaction, these two values may differ from each other.

If the original crack has propagated with two branching cracks, as shown in Fig. 3(b), the fictitious stresses σ and τ on the surfaces of the original crack, generated by the applied boundary loads, result in an opening force O and a sliding force S on the branching cracks.

In the case of different orientations of random cracks, the normal stress σ may be positive or negative with consideration of different lateral stresses, although the major stress is tensile

$$O = \begin{cases} a_i(-\tau \sin \theta_{ij} + \sigma \cos \theta_{ij}), & \text{for } \sigma > 0 \\ a_i(-\tau \sin \theta_{ij} + \sigma \lambda |\sin \theta_{ij}|), & \text{for } \sigma < 0 \end{cases}; \quad S = a_i(\tau + \sigma \lambda) \cos \theta_{ij} \tag{13}$$

where λ is the friction coefficient between the two crack surfaces in compression. When the normal stress is positive, the frictional term in the above equation is absent.

For the computation of the SIFs at each tip of the branching crack, an analogous problem (where an opening force and a sliding force act on a crack surface) has to be considered:

$$K_I^A = \frac{1}{2\sqrt{\pi a}} \left[P \sqrt{\frac{a+b}{a-b}} + Q \left(\frac{c-1}{c+1} \right) \right], \quad K_{II}^A = \frac{-1}{2\sqrt{\pi a}} \left[P \left(\frac{c-1}{c+1} \right) - Q \sqrt{\frac{a+b}{a-b}} \right] \tag{14}$$

The constant c depends on the material properties and the stress state in the specimen. In the case of a pair of forces, and specially for the problem shown in Fig. 3(b), with the fictitious normal stress σ_n and shear stress σ_t on the branching cracks, the SIFs at the tip are evaluated from

$$K_I = \frac{O}{\sqrt{\pi b_i}} + \sigma_n \sqrt{\pi b_i}, \quad K_{II} = \frac{S}{\sqrt{\pi b_i}} + \sigma_t \sqrt{\pi b_i} \tag{15}$$

where b_i is the length of the branching crack.

If σ_n is positive, the propagation length should be determined from

$$\frac{a_i(-\tau \sin \theta_{ij} + \sigma \cos \theta_{ij})}{\sqrt{\pi b_i}} + \sigma_n \sqrt{\pi b_i} = K_{IC} \tag{16}$$

The solution of Eq. (16) can be expressed in compact form:

$$\frac{A}{x} + Bx = K_{IC} \tag{17}$$

where $x = \sqrt{\pi b_i}$ ($x \geq 0$). The solution can be obtained by the intersections of the curve and the straight line in Fig. 4. It can be seen from Fig. 4 that there may be three different situations for the solution of the branching crack.

If the values of A and B satisfy the condition $4AB < K_{IC}^2$, the length of the branching crack presents two positive roots. The smaller should be taken as the true solution since the branching crack propagates progressively from zero to a relatively stable value, for which a small increment of the length will cause a decrease of the SIFs.

The values of A and B increase with the increment of the applied loads, and the propagation

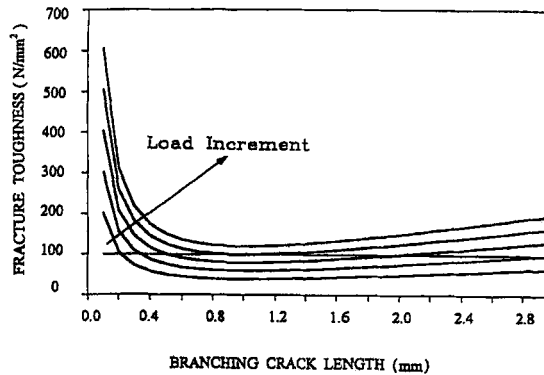


Fig. 4. Variation of the branching crack length with load increment.

length of the branching crack will increase progressively. The critical condition will occur when $4AB = K_{IC}^2$ (only one intersection exists).

The propagation of the branching crack will become unstable if $4AB > K_{IC}^2$ (there is no intersection in this case).

It can be demonstrated that there is a relatively stable stage of microcrack propagation in brittle specimen even under prevailing tension if the external stresses are not too high.

Specimen in compression

If the major stress is compressive, the fictitious normal stress on the original crack is negative in most cases,

$$S = \begin{cases} a_i(\tau + \sigma\lambda) \cos \theta_{ij}, & \text{for } \tau > 0 \\ a_i(\tau - \sigma\lambda) \cos \theta_{ij}, & \text{for } \tau < 0 \end{cases}; \quad O = a_i(-\tau \sin \theta_{ij} + \sigma\lambda |\sin \theta_{ij}|) \quad (18)$$

If the fictitious normal stress on the branching crack is also negative, from the relationship

$$\frac{a_i(-\tau \sin \theta_{ij} + \sigma |\sin \theta_{ij}|)}{\sqrt{\pi b_i}} = K_{IC} \quad (19)$$

we know that the propagation of the branching crack is stable, so that its length can be obtained step by step along with the increase of the applied external loads on the specimen.

CRACK PROPAGATION ARREST AND SPECIMEN FAILURE

During crack propagation, some branching cracks may intersect with other cracks. When the intersection takes place, two cases are possible in computer simulation within a certain load increment. The first case is that the propagating crack tip is very close to another crack within a given distance (in computation we use 0.1 mm); the second case is where the propagating crack tip passes across another crack. From experimental observations, we know that some minor cracks will stop propagating when they intersect with other cracks. Therefore, for each load increment, we compute the new positions of the propagating crack tips; if an intersection occurs, the shorter branching crack will stop propagating, whereas the longer can continue propagating in the next

load increment. In the case of two branching cracks passing across each other, the length of the shorter branching crack should be updated by the intersection position.

Since the algorithm used in this study is in load control, the failure of a specimen should be checked in each load increment. There are many crack intersections formed during crack propagation in very dense microcrack arrays, and many intersections even coalesce with each other. So it is rather difficult to identify how many independent intersection groups exist in a certain load step. A special coalescence matrix is adopted to identify the independent coalescence groups. The element $c_{i,j}$ in a coalescence matrix represents the intersection state between microcracks i and j , the value is taken as "1" or "0" according to their relative positions. If the value is "1", it means that microcrack i intersects with microcrack j . From the values of elements in this matrix, different independent intersection groups can be determined, and each group will be checked against the failure of the specimen. The corresponding failure criterion requires an independent crack coalescence group intersecting two external boundary elements; in this case this group is assumed as the fatal coalescence cluster.

EXAMPLES

To illustrate some features of the proposed numerical model, two examples are shown with random interacting microcracks in a finite sized specimen.

The first example is a 100 mm by 100 mm square plate in tension, with 50 random pre-existing microcracks with Uniform Distributions in position, length and orientation. The material parameters are: Young's modulus $E = 30,000 \text{ N/mm}^2$, Poisson ratio $\nu = 0.3$, Fracture Toughness $K_{IC} = 20 \text{ N/mm}^{3/2}$. The primitive crack distribution is shown in Fig. 5. The computed failure stress is 3.5 N/mm^2 , which is very close to the normal strength of a brittle material with the same material parameters. The damage process during the loading increment is shown in Fig. 6.

The second example is given by the same specimen but in compression, with the primitive crack distribution assumed to be as in example 1. The crack pattern during the loading process is shown in Fig. 7. The computed failure load is -15 N/mm^2 (more than 4 times that in tension). In brittle materials, compressive strength is much higher than that in tension, and this well-known phenomenon can be easily explained with the interaction, propagation and coalescence behaviour of pre-existing microcracks.



Fig. 5. Primitive crack distribution in a specimen.

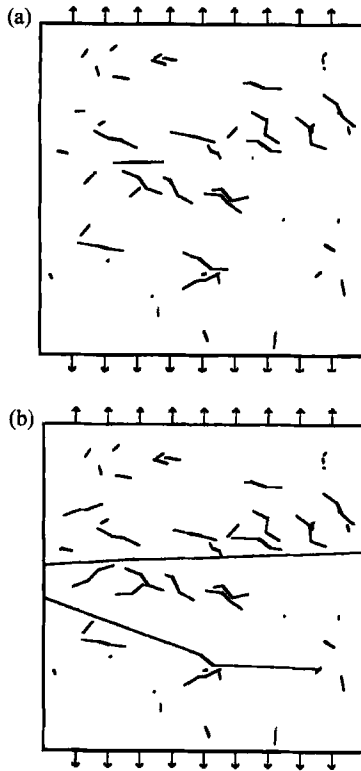


Fig. 6. Crack behaviour under tensile loading. (a) Crack propagation at 3.0 N/mm^2 , (b) Crack pattern at failure, 3.5 N/mm^2 .

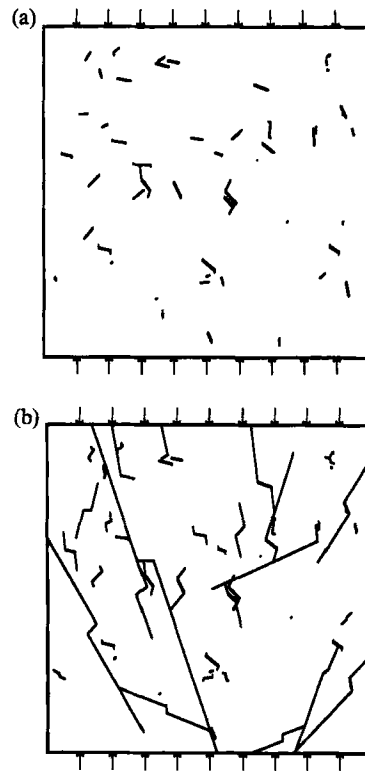


Fig. 7. Crack behaviour under compressive loading. (a) Crack propagation at -12.0 N/mm^2 , (b) Crack pattern at failure, -15.0 N/mm^2 .

CONCLUDING REMARKS

An attempt to study the damage accumulation process in brittle materials is made in this paper, based on the simulation of the coupling between crack interactions, crack propagation and finite-size boundary influences.

The boundary element method is introduced to take account of the effects of finite-size boundaries. A coalescence criterion is proposed to rule the intersection behaviour and to describe the arrest of the less important intersecting cracks. The failure of the specimen is accomplished with a characteristic coalescence matrix which can identify the fatal coalescence cluster out of many intersections of propagating microcracks.

With the present numerical model, it is easy to simulate the damage process in a brittle specimen, with any configuration and statistical distribution of random microcracks, under arbitrary plane stress conditions.

REFERENCES

1. H. Horii and S. Nemat-Nasser (1986) Brittle failure in compression: splitting, faulting and brittle-ductile transition. *Phil. Trans. R. Soc. London* **A319**, 337–374.
2. M. Kachanov (1987) Elastic solids with many cracks: a simple method of analysis. *Int. J. Solid Struct.* **23**(1), 23–43.
3. L. R. F. Rose (1986) Microcrack interaction with a main crack. *Int. J. Fract.* **31**, 233–242.

4. Guo-ping Yang and Xila Liu (1993) Interaction and propagation of random microcracks in compression. *Studi e Ricerche, Italy* **14**, 121–141.
5. A. Carpinteri and Guo-ping Yang (1996) Fractal dimension evolution of microcrack net in disordered materials. *Theoret. Appl. Fract. Mech.* **25**, 73–81.
6. I. N. Sneddon and M. Lowengrub (1969) *Crack Problems in The Classical Theory of Elasticity*, John Wiley & Sons Inc, 29–40.
7. Guo-ping Yang and Xila Liu (1991) Microcrack interaction in concrete, *Proc. of Intl. Symp. on Concrete Engng.*, Nanjing, 186–193.
8. S. L. Crouch and A. M. Starfield (1983) *Boundary Element Methods in Solid Mechanics*, George Allen and Unwin, London.
9. A. Carpinteri, C. Scavia and Guo-ping Yang (1996) Microcrack propagation, coalescence and size effects in compression. *Engng Fract. Mech.* **54**, 335–347.